Reactive and Functional Polymers 136 (2019) 25–33

Contents lists available at ScienceDirect

Reactive and Functional Polymers

journal homepage: www.elsevier.com/locate/react

Antimicrobial coating of textiles by laccase *in situ* polymerization of catechol and *p*-phenylenediamine

Jing Su[a,b], Jennifer Noro[b], Sónia Silva[b], Jiajia Fu[a], Qiang Wang[a], Artur Ribeiro[b], Carla Silva[b,**], Artur Cavaco-Paulo[a,b,*]

[a] International Joint Research Laboratory for Textile and Fiber Bioprocesses, Jiangnan University, Wuxi 214122, China
[b] Centre of Biological Engineering, University of Minho, Campus de Gualtar, 4710-057, Braga, Portugal

ARTICLE INFO

Keywords:
Poly(catechol)
Poly(*p*-phenylenediamine)
Textile fibers
Antimicrobial

ABSTRACT

Textile fabrics made up of cotton, wool, and polyethylene terephthalate (PET) were coated with poly(catechol) and poly(*p*-phenylenediamine) through the *in situ* enzymatic polymerization of catechol and *p*-phenylenediamine, assisted by laccase under high-pressure homogenization. All coated fabrics showed antimicrobial activity against both gram-positive (*Staphylococcus aureus*) and gram-negative (*Escherichia coli*) strains and revealed antioxidant character, measured in terms of ($ABTS^{\bullet+}$)-scavenging activity. The coating of PET and cotton fabrics with both polymers did not affect the viability of foreskin fibroblasts. The methodology proposed for the *in situ* coating of textile materials assisted by laccase showed to be a promising approach to produce colored antimicrobial textiles with vast potential applications, namely, clothing and medical devices, among others.

1. Introduction

Fiber-based textile materials have been used for various purposes such as clothing, domestic home furnishings, food packaging, sport equipment, medical devices, healthcare, and hygienic applications [1]. The large surface area and capacity to retain moisture enable the growth of microorganisms on these textile structures, hence causing a range of undesirable effects to textiles and users and becoming a health and safety issue [1]. To minimize these problems, vast research has been undertaken on the development of different methods of protection of textile surfaces against microbial growth [2–7]. General approaches for preserving surfaces from antimicrobial growth include the incorporation of antibiotics, silver and copper nanoparticles, and/or other biocidal agents [8,9]. Despite their efficacy, these methods present several adverse effects including risk for the users and environmental risk during long-term use, among others [3,10]. The search for new, efficient, and safer antimicrobial technologies is thus imperative to face these drawbacks. Green technologies have been evaluated to pursue the production of multifunctional textile materials. Several compounds including quaternary ammonium salts, triclosan, metals, and metallic salts are used as coating materials to confer antimicrobial properties to the textile substrates [7,11–14]. The affinity of these compounds to fibers might be achieved by either physical or chemical grafting, which is dependent on the interactions between the compounds and the type of fiber used as the substrate [1,10].

Polyphenols are secondary metabolites ubiquitously distributed in higher plants, with significant roles as defense against plant pathogens and animal herbivore aggression and as response to various abiotic stress conditions such as rainfall and ultraviolet radiation [15]. Their protective activity has been attributed initially to their antioxidant, free radical scavenger, and metal chelator properties, to the capability of inhibiting or reducing different enzymes, and to their interaction with signal transduction pathways and cell receptors [15,16]. For all these reasons, these compounds have been evaluated for their biological properties and potential therapeutic behavior against several diseases [17–19]. They are also considered as powerful antimicrobial agents against gram-positive and gram-negative bacteria, as they do not exhibit the side effects often associated with synthetic chemicals [1]. Moreover, these compounds are also presented as an environmentally friendly alternative for the production of antimicrobial substrates.

Abbreviations: S. aureus, *Staphylococcus aureus*; *E. coli*, *Escherichia coli*; PET, polyethylene terephthalate; DLS, dynamic light scattering; ABTS, 2,2′-azinobis-(3-ethylbenzothiazoline-6-sulfonic acid); DMEM, Dulbecco's modified Eagle's medium; DMSO, dimethyl sulfoxide; DP, the polymerization degree; SEM, scanning electron microscopy; EDS, energy-dispersive X-ray spectroscopy; FTIR, Fourier-transform infrared spectroscopy; TGA, thermogravimetric analysis

* Corresponding author at: International Joint Research Laboratory for Textile and Fiber Bioprocesses, Jiangnan University, Wuxi 214122, China.
** Corresponding author.
E-mail addresses: carla.silva@ceb.uminho.pt (C. Silva), artur@deb.uminho.pt (A. Cavaco-Paulo).

https://doi.org/10.1016/j.reactfunctpolym.2018.11.015
Received 8 October 2018; Received in revised form 19 November 2018; Accepted 21 November 2018
Available online 02 December 2018
1381-5148/

However, despite the advantages already reported, the mechanism of antimicrobial activity has not been fully understood thus far because of their structure complexity.

Previous findings reveal that laccase, native or chemically modified, is able to efficiently oxidize phenolic compounds such as catechol and *p*-phenylenediamine monomers [20]. Our data showed that, although the role of PEG in enzymatic polymerization has not been clearly understood, the PEGylated enzyme form was more prone to produce higher amount and longer polymers than the native enzyme form [21]. The PEGylated enzyme form was therefore considered to conduct the polymerizations in the present study.

Herein, three different fabric substrates (PET, cotton, and wool) were coated *in situ* with laccase-oxidized poly(catechol) and poly(*p*-phenylenediamine) under high-pressure homogenization (HPH). The fabrics served simultaneously as enzyme containers and coating substrates. The polymerization of both monomers was followed in solution by UV–Visible spectroscopy, and the new oligomers/polymers formed were characterized by ^{1}H NMR, MALDI-TOF spectroscopy and dynamic light scattering (DLS). The coating efficiency was evaluated by fabric spectral value determination (checksum *K/S*) and scanning electron microscopy (SEM). The antioxidant activity of the powders produced was investigated using the $ABTS^{\bullet+}$ scavenging activity methodology. The antimicrobial activity of the coated fabrics was evaluated against both the gram-positive *Staphylococcus aureus (S. aureus)* and the gram-negative *Escherichia coli (E. coli)* strains using the quantitative methodology. The cytotoxicity of the coated substrates was evaluated by exposing skin fibroblasts to culture media preconditioned by contact with the fabrics.

2. Experimental

2.1. Materials

Laccase from *Myceliophthora thermophila* was supplied by Novozymes, Denmark. Catechol, *p*-phenylenediamine, poly(ethylene glycol) methyl ether, sodium carbonate, 95% ethanol, Folin–Ciocalteu reagent, 2,2′-azinobis-(3-ethylbenzothiazoline-6-sulfonic acid), and potassium persulfate were purchased from Sigma-Aldrich, Spain. Deuterated dimethyl sulfoxide was obtained from Cortecnet, France. BJ-5ta cell line (normal human skin fibroblasts immortalized by overexpression of telomerase) was purchased from American Type Culture Collection (ATCC). Dulbecco's modified Eagle's medium (DMEM) was purchased from Biochrom, UK. Medium 199, penicillin/streptomycin, and Hygromycin B were obtained from Sigma-Aldrich, Spain. Fetal bovine serum (FBS) was purchased from GRISP, Portugal. The gram-positive *S. aureus (*ATCC 6538*)* and gram-negative *E. coli (*CECT 434) strains were obtained from ATCC and from Spanish Type Culture Collection. Trypticase soy broth (TSB) and trypticase soy agar (TSA) were purchased from Liofilchem, Italy.

The fabrics used for the study were supplied by a textile company, and they had the following characteristics: polyethylene terephthalate (PET): 96 g/m^2, 24*40 yarns/cm^2; cotton: 65 g/m^2, 35*40 yarns/cm^2; and wool: 420 g/m^2, 15*15 yarns/cm^2.

The HPH device used for the experiments was EmulsiFlex C3, with a constant flow-through capacity of 3 L/h and the ability to process 10 mL of samples; the homogenizing pressure is adjustable between 500 and 30,000 psi or 35 and 2000 bar, and the flow rate is independent of pressure.

2.2. Physicochemical characterization

2.2.1. PEGylation of laccase

Laccase from *M. thermophila* was PEGylated as previously reported [21] using the procedure of Daly et al. [22].

2.2.2. Enzymatic-assisted polymerization of catechol and *p*-phenylenediamine

Catechol and *p*-phenylenediamine polymerization was processed by the method reported previously [20] by incubating 50 mM of each monomer with PEGylated laccase (100 U/mL) in acetate buffer (pH = 5). The enzyme was confined in bags of polyethylene glycol (PET), cotton, and wool, and the bags were placed in the sample receptor of the HPH device. Afterwards, the monomer solution was added, and the homogenization proceeded for 2 h (corresponding to 360 homogenization cycles). The starting temperature was set to 40 °C, and the inherent increase of temperature during the high-energy processing was monitored. Further, the polymer powder was collected from the HPH device by dissolution with dimethyl sulfoxide to solubilize the insoluble polymers and was posteriorly dried under vacuum for characterization.

2.2.3. UV–Visible spectral analysis

The polymerization was followed by UV–Visible spectroscopy using a 96-quartz microplate reader (BioTek Synergy Mx, Shimadzu, Japan).

2.2.3.1. ^{1}H NMR spectroscopy. The precipitates obtained after washing and centrifugation were dissolved in deuterated solvent, DMSO-d_6, for ^{1}H NMR evaluation. The spectra were acquired using Bruker Avance III 400 (400 MHz) using the peak solvent as an internal reference standard.

2.2.4. MALDI-TOF spectroscopy analysis

The polymers were analyzed by matrix-assisted laser desorption/ionization with time-of-flight (MALDI-TOF) using 2,5-dihydroxybenzoic acid (DHB) as the matrix (≥99.5%). The mass spectra were acquired using an Ultra-flex MALDI-TOF mass spectrophotometer (Bruker Daltonics GmbH) equipped with a 337 nm nitrogen laser. For this purpose, the samples were dissolved in TA30 (30% acetonitrile/70% TFA) solution and mixed with a 20 mg/mL solution of DHB (1:1). Then, a volume of 2 μL was placed on the ground steel plate (Bruker part no. 209519) until dry. The mass spectra were acquired in linear positive mode.

The Mn (number-average molecular weight) and Mw (weight-average molecular weight) of polycatechol obtained after oxidation were calculated as follows:

$$Mn = \frac{\sum n_i M_i}{\sum n_i};\ Mw = \frac{\sum n_i M_i^2}{\sum n_i M_i};\ PDI = \frac{M_w}{M_n};$$

where n_i is the relative abundance of each peak, M_i is the *m/z* corresponding to each peak, and PDI is the polydispersity.

2.2.5. Determination of total content of free OH groups

The total content of free OH groups was determined before and after polymerization using the Folin–Ciocalteu spectrophotometric method. The monomer and polymer solutions dissolved in DMSO (100 μL) were added to the mixture of Folin–Ciocalteu reagent (500 μL) and distilled water (6 mL), and the mixture was shaken for 1 min. Afterwards, a Na_2CO_3 solution (15 wt%, 2 mL) was added to the mixture and shaken for 1 min. Later, the solution was brought up to 10 mL by adding distilled water. After 2 h, the absorbance was measured at 750 nm (25 °C). The total content of free OH was assessed by plotting a gallic acid calibration curve (from 1 to 1500 μg/mL). The equation of the gallic acid calibration curve was A = 0.2977c + 0.0368, and the correlation coefficient was r^2 = 0.999.

2.2.6. Fourier-transform infrared spectroscopy analysis of powder polymers

Infrared spectra were recorded on a Fourier-transform infrared spectroscopy (FT-IR) Bomem MB using NaCl cells and Nujol. The spectra were recorded in the absorption mode in the range of 4000–500 cm^{-1}, with a 4 cm^{-1} resolution.

2.2.7. Thermogravimetric analysis of powder polymers

Thermogravimetric analysis (TGA) was performed in PerkinElmer TGA 4000. The calibration curve was plotted for metals such as nickel, Alumel, and Perkalloy, based on their Curie point reference. The temperature range was 30–700 °C (heating rate of 20 °C/min, sample weight: 12–16 mg), and the nitrogen flowrate was 20 mL/min (3 bar).

2.2.8. Scanning electron microscopy

The surface topography and chemical composition of the coated samples were investigated by SEM/energy-dispersive X-ray spectroscopy (EDS) evaluation. All the fabric samples were added to aluminum pin stubs with an electrically conductive carbon adhesive tape (PELCO Tabs™), with the excess removed using compressed air. Samples were coated with 2 nm of Au for improved conductivity. The aluminum pin stub was then placed inside a Phenom Standard Sample Holder, and different points for each sample were analyzed for elemental composition. The samples were characterized using a desktop scanning electron microscope coupled with EDS analysis (Phenom ProX with EDS detector; Phenom-World BV, The Netherlands). All results for the quantification of the concentration of the elements present in the samples were acquired using ProSuite software integrated with Phenom Element Identification software, expressed in either weight or atomic concentration.

2.2.9. (ABTS·+)-scavenging activity of polymer powders

ABTS radical cation ($ABTS^{\bullet+}$)-scavenging activity was determined according to the method described by Re et al. with some modifications [23]. ABTS was produced by reacting 7 mM ABTS and 2.45 mM potassium persulfate in 10 mL of demineralized water in an Erlenmeyer flask, with magnetic stirring, in the dark at 26 ± 3 °C for 12–16 h. An aliquot of blue–green ABTS solution was then diluted with 95% ethanol to give an absorbance of 0.7 ± 0.02 at 734 nm. For this, ABTS adjusted solution (20 µL) and ethanol (500 µL) were mixed in an Eppendorf tube, and then, 200 µL of the mixture was taken to read the absorbance at 734 nm corresponding to the blank control (E1) (Spectronic Genesys 5, Germany). The test polymer solutions with different concentrations (5, 50, 100, 200, 400, 600, 800, and 1000 µg/m L) were analyzed. The absorbance of the reaction mixture was measured after 6 min (E2), and a control mixture without the polymer solution was also measured. The ($ABTS^{\bullet+}$)-scavenging activity was assessed by plotting a Trolox calibration curve (from 1 to 1000 µg/mL). The equation of the Trolox calibration curve was A = 0.1078c + 10.514, and the correlation coefficient was $r^2 = 0.9879$. The ($ABTS^{\bullet+}$)-scavenging activity (%) was calculated as follows:

$$(ABTS^{\bullet+}) - scavenge\ (\%) = \left(\frac{E1 - E2}{E1}\right) \times 100$$

2.2.10. Antimicrobial activity of coated fabrics

The antimicrobial activity of the coated fabrics was evaluated against the gram-positive *S. aureus* (ATCC 6538) and gram-negative *E. coli* (CECT 434) strains using the quantitative method based on the AATCC Test 100–2004 protocols (AATCC 100 2004: Antimicrobial Activity Assessment of Textile Materials: Parallel Streak Method from American Association of Textile Chemists and Colorists) with some modifications. The fabric swatches were previously sterilized under UV for 30 min. Each strain was incubated with TSB inoculum for 24 h at 37 °C. The bacteria concentration was adjusted with TSB to 2 × 105 cells/mL. Then, 4 mL of each diluted inoculum was placed in each textile square sample of size 0.5 × 0.5 cm. The samples were incubated for additional 24 h at 37 °C. After the incubation period, 10 mL of 0.1 M PBS (physiological buffer solution) was added and the samples homogenized in the vortex. To determine the number of living bacteria, the serial dilution plate count method was performed. TSA agar plates were incubated for 24 h at 37 °C, and the total CFUs were enumerated. All the assays were performed in duplicate and repeated three times.

2.2.11. Washing fastness of coated fabrics

The washing fastness of the coated fabrics with both poly(catechol) and poly(*p*-phenylenediamine) was evaluated. For this purpose, the samples were washed five times (each washing for 30 min.) at 50 °C with a detergent solution (0.5%). After each washing, the solutions were collected for UV–Visible spectra evaluation, and after the fifth washing, the spectra values (*K/S*) of the fabric samples were determined.

2.2.12. Evaluation of potential cytotoxicity of fabrics

2.2.12.1. Cell culture. The BJ-5ta cell line (normal human skin fibroblasts immortalized by overexpression of telomerase) was maintained according to ATCC recommendations (four parts of DMEM containing 4 mmol/L-glutamine, 4.5 g/L sodium bicarbonate and 1 part of Medium 199, supplemented with 10% (*v*/v) of FBS, 1% (v/v) of penicillin/streptomycin solution, and 10 µg/mL Hygromycin B). Cells were maintained at 37 °C in a humidified atmosphere with 5% CO_2, and culture medium was replaced every 2 days.

2.2.12.2. Cytotoxicity evaluation. BJ-5ta cells were used as a model of general cytotoxicity. Cytotoxicity induced by bioactive leaching substances, which diffused from the raw fabrics and from the fabrics made up of poly(catechol) and poly(*p*-phenylenediamine), was evaluated by exposing cells to the culture medium conditioned by 24 h contact with the fabrics. The fabrics were sterilized by UV for 30 min prior incubation with the culture media. The conditioned media were obtained by incubating the sterilized fabrics in 2 mL of medium at 37 °C in a humidified atmosphere of 5% CO_2 for 24 h.

Cells were seeded at a density of 10×10^3 cells/100 µ L/well on 96-well tissue culture polystyrene plates (SPL Life Sciences, South Korea) the day before experiments and then exposed to the conditioned medium, undiluted and diluted as 1:2 or 1:10, whenever necessary and were further incubated at 37 °C in a humidified atmosphere of 5% CO_2. At the end of 24 and 48 h of contact, the metabolic viability was assessed using the Promega CellTiter 96® AQueous Non-Radioactive Cell Proliferation (MTS) assay (Promega, USA).

2.2.13. Statistical analysis

Data are presented as average standard deviation (SD) ($n = 3$). Statistical comparisons were performed using one-way ANOVA with GraphPad Prism 5.0 software (La Jolla, CA, U.S.A.). Tukey's *post hoc* test was used to compare all the results between them, and Dunnet's test was used to compare the results with a specific control. A p value of < 0.0001 was considered to be statistically significant.

3. Results and discussion

3.1. Polymer characterization

3.1.1. UV–Visible spectroscopy

The polymerization of catechol and *p*-phenylenediamine by PEGylated laccase under HPH was followed during time by UV–Visible spectroscopy. During polymerization, all the catechol reaction mixtures changed from colorless to light/dark brown, as can be seen by the typical peak around 300 nm, which increased with time, because of the soluble oligomers and polymers formed. Additionally, a new peak appeared at around 430 nm, thus confirming the polymerization of catechol. This peak was more pronounced when wool fiber was used as the enzyme container because of the higher amount of soluble oligomers formed (Fig. 1A). The *p*-phenylenediamine mixtures changed from colorless to light/dark purple during the oxidation process. The spectra of poly(*p*-phenylenediamine) presented, however, a different feature compared with poly(catechol) and showed two characteristic peaks at around 350 and 520 nm, attributed to the new polymers formed [24]. The absorbance did not show significant differences depending on the enzyme bag container used (Fig. 1B).

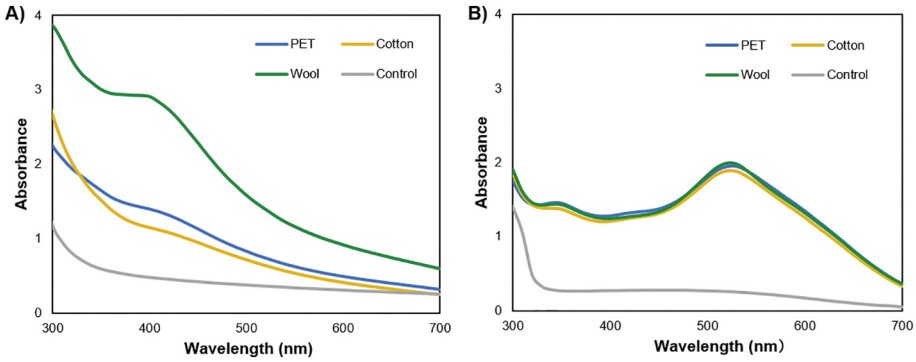

Fig. 1. UV–Visible spectra of soluble oligomers/polymers after 2 h of polymerization with PEGylated laccase contained in different bags (PET, cotton, and wool): A) poly(catechol); B) poly(*p*-phenylenediamine); the control samples correspond to the monomer spectra before mixture into the cup container of the homogenizer.

It is noteworthy that the temperature was controlled during processing reaching maximum levels of 60 °C and the activity of the enzyme was monitored with progression of time. Despite the decrease in activity observed (data not shown), the polymerization of both monomers was not hampered because it occurs in the first 0.5–1 h of incubation [25].

3.1.2. Polymer powder characterization: amount of polymer, particle size, and total content of free OH groups

Both soluble and insoluble oligomers/polymers were collected and quantified after freeze-drying. For catechol and comparing the oligomers/polymers produced using the three fabrics as containers, conversion yields of approximately 70% were obtained. The conversion levels obtained for poly(*p*-phenyenediamine) were higher, reaching values up to 95%. These findings confirm that, despite the different polymer sizes obtained, the conversion rates were not dependent on the type of enzyme container used but on the type of monomer. The polymerization degree (DP) of oligomers/polymers was calculated based on ^{1}H NMR and MALDI-TOF analyses. As it can be seen in Table 1, when PET and cotton were used as enzyme containers for catechol polymerization, a DP of 10 is achieved. When wool was used as a container, the DP obtained was lower, which is in accordance with the higher amount of soluble oligomers evaluated by UV–Visible spectroscopy. In the case of poly(*p*-phenylenediamine), similar DPs were obtained when using PET and wool, DP = 12 and DP = 11, respectively. When cotton was used, slightly smaller polymers were produced. These findings are most likely related to the amount of insoluble oligomers/polymers rather than to the amount of soluble ones, as similar spectra have been observed for all the samples using the different enzyme containers. To evaluate the role of the different enzyme containers on the polymerization of both monomers, the amount of oxyphenylene units was estimated by measuring the total content of free OH in all the mixtures after reaction (Table 1). The data obtained reveal that similar values were obtained for all the samples produced in the presence of the different containers, thus indicating that the type of fiber container does not influence the catalytic enzyme performance. One might speculate that the level of coating (discussed further) will be more dependent on the polymer particle size than on the molecular size of the polymers produced. Previously, we found that the PEGylated laccase form, contained inside a PET fabric, was able to produced polymers of poly(catechol) with a small size of approximately 30 to 60 nm, under HPH [25]. Herein, while small particle sizes were obtained for poly(catechol) oxidized by PEGylated laccase, this trend was not observed for the poly(*p*-phenylenediamine). The oxidation of *p*-phenylenediamine by PEGylated laccase gave rise to polymer particles of size up to 765 nm, as also confirmed by others [26].

3.1.3. FTIR and TGA

The confirmation of polymerization of both monomers was also made by FTIR and TGA of the final powders produced (Fig. 2). In the FTIR spectra corresponding to catechol (Fig. 2A1), two broad peaks can be depicted at 3448.47 cm^{-1} and 3321.18 cm^{-1}, which belong to the characteristic O—H vibration bands of the monomer. In the polymer spectra, these peaks are less intense, meaning that the polymerization occurred by the hydroxyl groups. The absorption peaks attributed to the aromatic ring C = C vibration bands between 1360 and 1600 cm^{-1} remain the same in both monomer and polymer spectra. In the FTIR spectra of poly(*p*-phenylenediamine) (Fig. 2A2), a decrease in the peak intensity corresponding to the amines (3400 cm^{-1}) can be observed, which confirm the proposed polymerization mechanism (Fig. 2C).

The thermal properties of poly(catechol) and poly(*p*-phenylenediamine) were investigated by TGA. As it can be seen in Fig. 2B, the

Table 1
Characterization of oligomers/polymers produced by *in situ* oxidation with PEGylated laccase under high-pressure homogenization and coating characterization.

		Polymer characterization					Coating characterization
Polymer	Fabrics	Conversion yield* (%)	DP[a]	Particle size[b]	PDI	Free OH content [c]	Coating yield (%)[Δ]
Poly(catechol)	PET	72.8	10	55.77 ± 1.60	0.11	0.3634	3.5
	Cotton	69.8	10	74.66 ± 3.55	0.11	0.3869	6.4
	Wool	71.8	7	37.09 ± 0.36	0.04	0.3802	1.3
Poly(*p*-phenylenediamine)	PET	84.8	12	683.80 ± 6.86	0.05	–	4.1
	Cotton	83.8	9	692.30 ± 5.23	0.02	–	8.1
	Wool	83.8	11	765.40 ± 7.14	0.20	–	1.5

[a] The average DP of poly(catechol) was calculated by ^{1}H NMR (based on the integration of the terminal OH peak with the aromatic peak protons) and that of poly(*p*-phenylenediamine) (Fig. S1) by MALDI-TOF (calculated from $Mw/M_{p\text{-phenylenediamine}}$) (Fig. S2).
[b] Particle was dissolved in 50% H_2O and 50% DMSO and measured by DLS (dynamic light scattering) in a Malvern Zeta-sizer (UK);
[c] The free OH content was evaluated as catechol 1.00 (100%);
* The conversion yield was determined by weighing the fabrics before and after coating and by weight of the final solution after freeze-drying;
Δ The coating yield was determined by weighing the fabrics before and after coating.

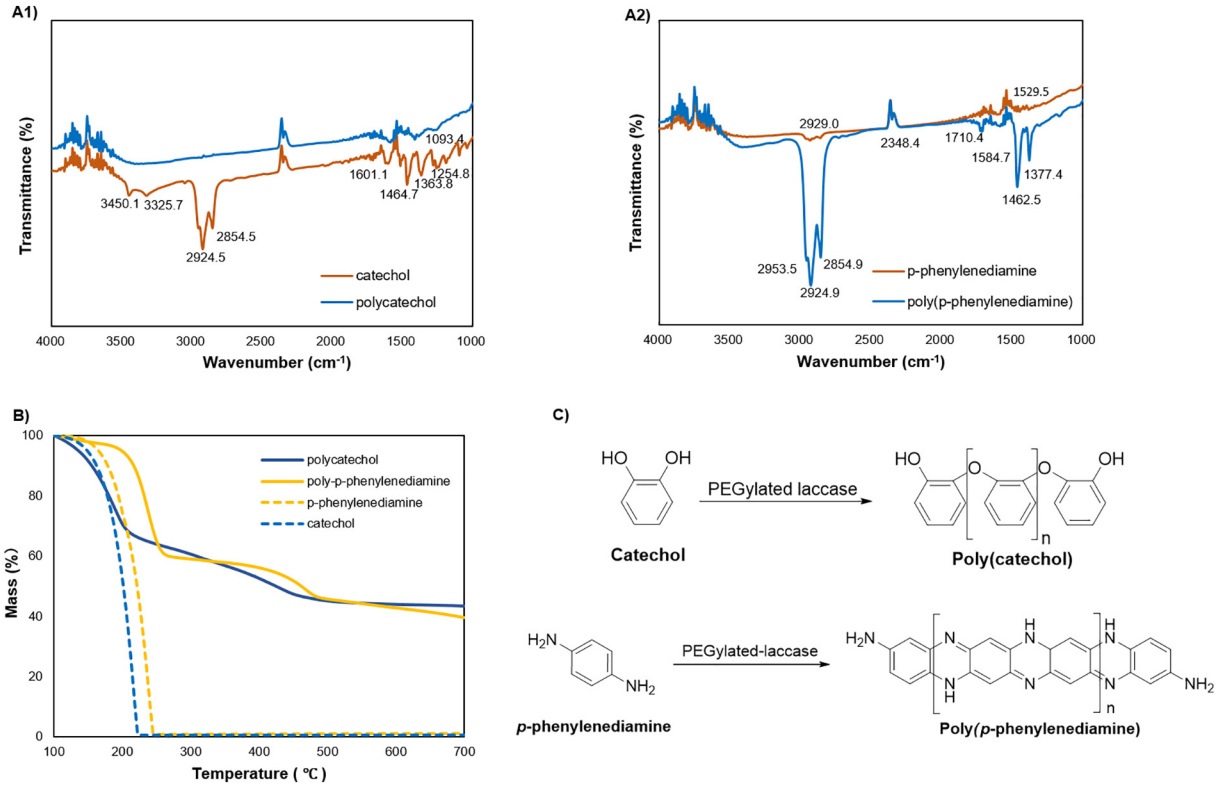

Fig. 2. FTIR and TGA of polymers: A1) poly(catechol); A2) poly(*p*-phenylenediamine); B) thermal performance of poly(catechol) and poly(*p*-phenylenediamine) and respective controls; C) schematic representation of polymerization mechanism of both polymers (upper scheme: poly(catechol); down scheme: poly(*p*-phenylenediamine).

monomers, catechol and *p*-phenylenediamine, all showed one-step decomposition, thus losing all the weight between 100 and 250 °C. The corresponding polymers have, however, a different thermal behavior. Poly(catechol) presented a very slow degradation rate at > 200 °C, thus showing two stages of weight loss, one at approximately 220 °C (35% of weight loss) and another at approximately 450 °C (55% of weight loss). Poly(*p*-phenylenediamine) presented a multistep decomposition thermal behavior differentiated from poly(catechol), with 40% of weight loss at approximately 250 °C and 55% of weight loss at 450 °C. Both polymers formed 40% of residue at approximately 700 °C, thus indicating a higher stability toward thermal degradation, which is in accordance with the results in previous studies [27–29]. The high amount of residue that remained on both polymers might be also attributed to the presence of fibrils on the samples, which have influenced the thermal behavior in the temperature range of 500–700 °C. The results correspond to the polymers produced using cotton as enzyme container, and this fiber presents this thermal behavior in specific experimental conditions [30].

3.1.4. Antioxidant activity

The exploitation of the radical-scavenging activity of different polyphenols has been undertaken by several researchers [31–34]. Their studies showed that the polymers have superior antioxidant properties compared to the respective monomers and that the antioxidant activity of the polyphenols will be dependent on the molecular mass and on the structure of the polymer.

In this study, the radical-scavenging activity of poly(catechol) and poly(*p*-phenylenediamine) was evaluated by the ABTS method, which has been applied to measure the total antioxidant activity of pure substance solutions, aqueous mixtures, and beverages [23]. The results in Fig. 3 demonstrate that, for both polymers, as the concentration of the test solution increased, their $ABTS^{\cdot+}$ scavenging ability increased, thus reaching a plateau above 600 µg/ml for the poly(catechol) and above 400 µg/ml for the poly(*p*-phenylenediamine). It is noteworthy that independent of the enzyme container used in the oxidation process, the powders produced displayed a similar antioxidant behavior for both polymers. The promising results obtained for the antioxidant analysis, might be a reliable indication that these polymers would confer antioxidant properties to the coated fabrics.

3.2. Coating characterization

3.2.1. Coating efficiency: coating yield and SEM visualization

The coating efficiency is expected to be dependent on several parameters including the type of monomer, the particle size of the forming polymer, and the type of fiber used as the container. The coating efficiency was, therefore, evaluated by measuring the coating yield by weighing the fabrics before and after coating and also by SEM examination. As can be seen in Fig. 4, the surfaces of the original PET (A1) and cotton (B1) are smooth and neat, whereas wool fibers (B3) present the typical scale-shape. Coated samples show macroscopic particles of both polymers attached to the fabric surfaces, as it can be seen by the coverage of the fiber surface (Fig. 4A2, A3, B2, B3 and C2, C3). The *in situ* polymerization of *p*-phenylenediamine gave rise to similar levels of coating (as highlighted in the figure at the bottom right corner), despite the differentiated spectra values obtained (see Table S1), which are related to the typical polymer coloration. The coating yield is related to not only the amount of polymer at the surface of the fibers evaluated by SEM but also the amount of small polymer particles that penetrate deeply inside the fibers, which also possess differentiated substantivity, and are not visible by spectroscopic evaluation nor by SEM. Moreover, it also depends on the substantivity of the polymer to each type of fiber. This explains the lower spectra results obtained for poly(catechol) when PET and cotton are used, which presented lower checksum *K/S*, revealing, however, similar coating yields. The higher wool coating levels observed for both polymers might be attributed to

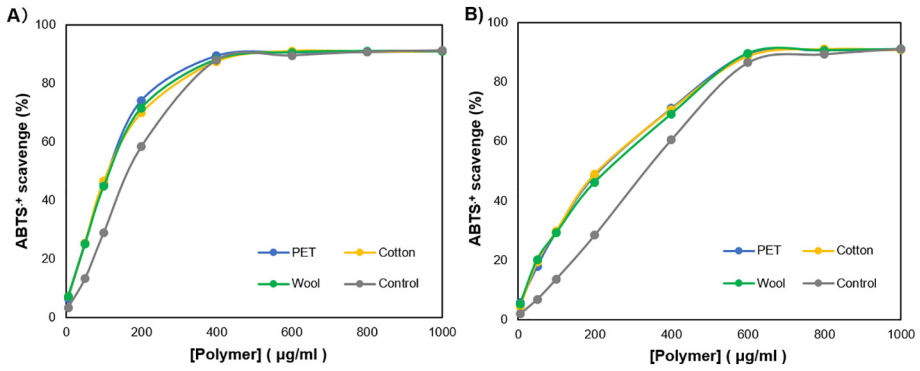

Fig. 3. ABTS$^{\cdot+}$ scavenge activity of fabrics coated after *in situ* coating with the enzymatically oxidized poly(catechol) and poly(*p*-phenylenediamine); A) fabrics coated with poly(catechol) using different fabric substrates as enzyme containers; B) fabrics coated with poly(*p*-phenylenediamine) using different fabric substrates as enzyme containers and its polymers on PET/cotton/wool; the positive control corresponds to Trolox.

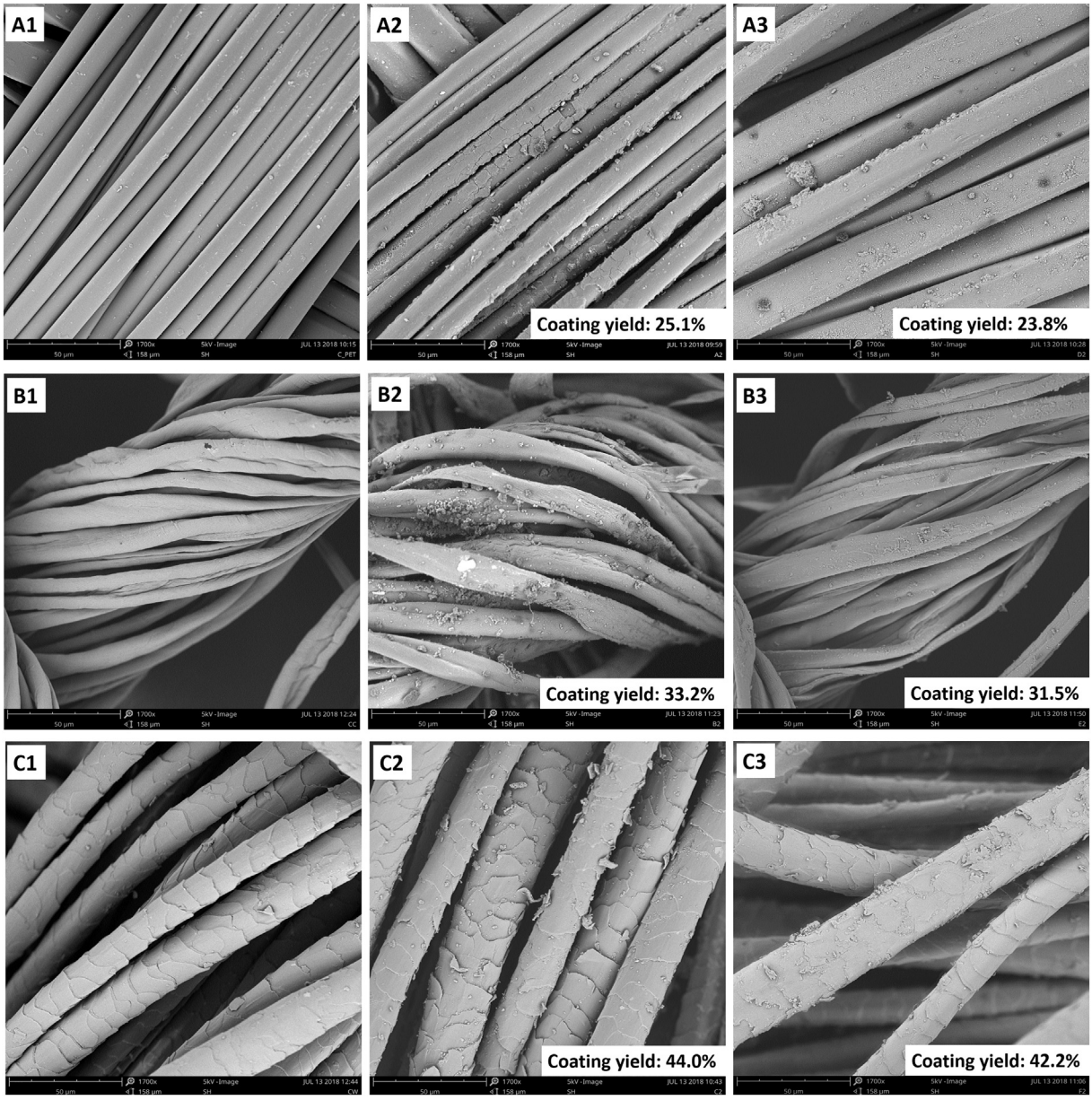

Fig. 4. SEM photographs of coated fabrics (×1700): A1: raw PET; A2: PET fabrics coated with poly(catechol); A3: PET fabrics coated with poly(*p*-phenylenediamine); B1: raw cotton; B2: cotton fabrics coated with poly(catechol); B3: cotton fabrics coated with poly(*p*-phenylenediamine); C1: raw wool; C2: wool fabrics coated with poly(catechol); C3: wool fabrics coated with poly(*p*-phenylenediamine); at the bottom right of each image is presented the coating yield calculated by weighing the fabrics before and after coating (the samples were placed in conditioned atmosphere for 24 h before weighing); the coating yield corresponds to the percentage of polymer formed that is coating the fabrics.

the higher fabric porosity of wool, which allowed higher polymer diffusion between fibers and thus higher polymer deposition inside yarns and in the outer fabric layer. Moreover, the scale-shape of this fiber is able to accumulate a higher amount of coated material than that of the plane and smooth PET and cotton fibers.

The homogenization process also contributed to the coating levels achieved by promoting homogenization of the solution, thus leading to a homogeneous coating. Further, the high pressures involved also allowed the penetration of the polymers more deeply inside the fibers.

The coating of fabrics with the produced polymers was also confirmed by EDS evaluation. The quantification of the elements present on the coated surface reveals the presence of carbon and oxygen on samples coated with poly(catechol) and the presence of carbon, oxygen, and nitrogen on samples coated with poly(*p*-phenylenediamine) (Table S2).

3.2.2. Antimicrobial activity of coated fabrics

Antibacterial performance ranks among the most attractive features of the fabrics modified with polyphenols and polyamino-phenols. According to the requirements of the standard procedures, antibacterial activities of the front and back sides of the studied materials should to be determined because of the fact that only marginal differences in growth were observed on both sides of poly(catechol)- and poly(*p*-phenylenediamine)-coated fabrics by a quantitative method for gram-positive *S. aureus* and gram-negative *E. coli*.

For a higher accuracy of the percentage of microbial growth inhibition, the quantitative method, AATCC Test Method 147–4004, was conducted to study the antimicrobial performance of the coated samples. This method provides values of antimicrobial activity on the basis of the reduction in planktonic bacterial growth [35,36].

As shown in Fig. 5, for both polymer-treated fabrics, the number of gram-positive and gram-negative bacteria decreased significantly compared with that in the noncoated samples (control). A higher bacterial reduction can be observed for wool fabrics coated with poly(catechol), thus revealing the highest antimicrobial activity with approximately to 2 log reduction compared to control ($p < .0001$) for both bacteria. This is related to the diffusivity of the material from the fabrics during testing. In fact, the wool samples coated with poly(catechol) presented lower fastness than PET and cotton samples (Table S1), which is directly associated with a higher amount of polymer that can be detached from the wool surface and act as an antimicrobial agent. When observing the sample photographs (Table S1), this behavior would be expectable because a higher coloration of the wool fabrics was achieved; however, this coloration, and as mentioned previously, does not correspond necessarily to a higher amount of polymer deposited onto the fabric surface (a similar coating yield was observed). Moreover, the intrinsic antimicrobial properties of wool might have played together with the previous events, a synergistic effect of bacterial reduction [37].

PET- and cotton-coated samples displayed a similar antimicrobial behavior with approximately 1 log reduction for both bacteria, however, with lower bacterial reduction than wool. Despite the similar coating yields observed (Fig. 4), the amount of polymer available at the fabric surface is lower. This is corroborated by the spectral results, which were lower for these substrates. In both cases, the low particle size of the polymer formed allowed its deep penetration inside the fibers, and a low coloration of the fibers outside layer was achieved (Table S1). The type and fiber structure were, in this case, key factors for the different levels of diffusion of the antimicrobial polymer agent, which were higher on the more open wool structure.

Fig. 5B shows the antimicrobial performance of the fabrics coated with poly(*p*-phenylenediamine). All the coated substrates revealed a similar antimicrobial behavior toward both *S. aureus and E. coli*, with approximately 2 log reduction compared to control ($p < .0001$). The similar antimicrobial behavior is, in this case, more attributable to the type of polymer rather than to the level of coating or to the type of fiber coated. This polymer has known antimicrobial properties when the monomer acquires an incremented antimicrobial behavior when polymerized. Its ability to diffuse from the fabric to the medium makes it more available to coat the surface of the cell membrane, thus preventing the nutrients from entering the cell [38]. It can also diffuse into the cell and adsorb the electronegative substances in the cell and flocculate them. This causes disturbance in the normal physiological activities of the bacterial cell and results in cell death [39]. Moreover, the conductive behavior of these polymer might also cause cell death by disrupting microbial cell walls by electrostatic contact [40,41].

In fact, our data showed that these coated fabrics demonstrated significant antimicrobial activity (p value $< .0001$ and log reduction ≥ 1 to < 2) by direct contact with both gram-positive and gram-negative bacteria. It is important to address that the two types of bacteria differ in their cell wall, *i.e.*, gram-positive bacteria presents a continuous cell wall of a thick layer of peptidoglycan, whereas gram-negative bacteria show a noncontinuous cell envelope formed by a thin layer of peptidoglycan covered by an outer membrane. With these differentiation, the cell wall structure would be expected a distinct behavior in what concerns their susceptibility to antimicrobial agents [42], but curiously, this was not observed.

3.2.3. Evaluation of fabric potential cytotoxicity

The term “antibacterial” raises questions among wearers as to the compatibility of antimicrobial textiles worn next to the skin. The user of the textile products can therefore expect them to be safe in use and not to pose a health risk [1,43]. Ideally, a textile with a bioactive compound should not elicit an inflammatory response or demonstrate cytotoxicity, particularly when the active compound is released from the material [44]. Thus, it was imperative in this work to evaluate the cytotoxicity of the fabrics coated with both poly(catechol) and poly(*p*-phenylenediamine). When considering the tissue compatibility of textiles with antimicrobial coating, it is particularly important to determine whether potentially toxic cell substances (*i.e.*, bioactive leaching substances) could be released from the material during normal wear.

To evaluate the cytotoxicity induced by bioactive leaching

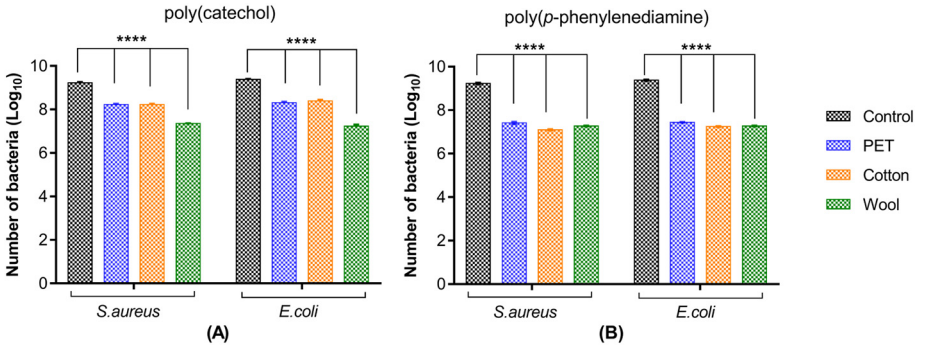

Fig. 5. Antimicrobial performance of fabrics treated with polymers using PEGylated laccase. (A): fabrics treated with poly(catechol) against *S. aureus* and *E. coli*; (B): fabrics treated with poly-*p*-phenylenediamine against *S. aureus* and *E. coli* (****: p value < 0.0001; N – number of bacteria); the control corresponds to the incubation of the noncoated samples (only one sample is represented, as all controls displayed similar results).

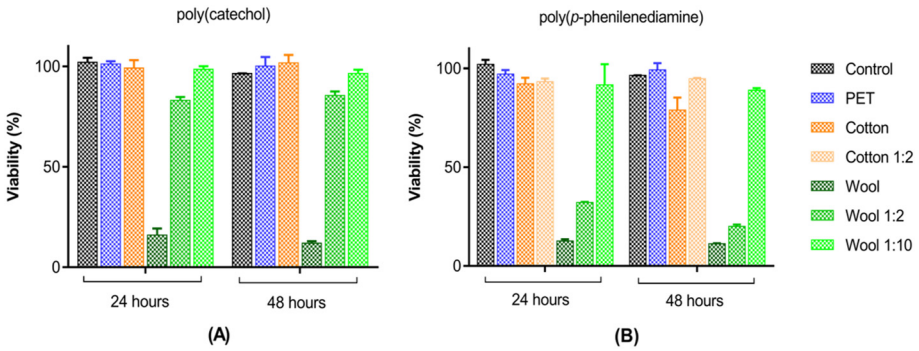

Fig. 6. BJ-5ta cell viability measured by MTS assay at 24 and 48 h of culture with undiluted conditioned media (PET, cotton, and wool) and with different dilutions of the conditioned media (cotton 1:2, wool 1:2, and wool 1:10) preconditioned for 24 h by contact with the raw fabrics and with the fabrics functionalized with poly(catechol) and poly(*p*-phenylenediamine). The data represent mean ± SD of two independent experiments, each with quadruplicates. **** $p \leq .0001$ when compared with the Life control. *** $p \leq .001$ when compared with the Life control.

substances, which diffused from the raw fabrics (PET, cotton, and wool) and the fabrics made up of poly(catechol) and poly(*p*-phenylenediamine), BJ-5ta fibroblasts were exposed to the culture medium preconditioned by contact with the fabrics for 24 h. Depending on the fabric, coating yield, and type of polymer, different diffusion rates were observed during the conditioning of the culture medium (Fig. S3). The degree of diffusion of the bioactive polymers from the fabrics was evaluated by direct observation of the color change of the conditioned culture media. This change was directly related to the amount of polymer diffused from the fabric to the medium. In general, higher diffusion rates were observed for the fabrics functionalized with the poly(*p*-phenylenediamine) polymer, with the highest diffusion being observed for wool. Depending on the degree of diffusion observed, the BJ-5ta cells were exposed to different dilutions of the conditioned medium (Fig. 6).

The results of the indirect contact study after fibroblast incubation for 24 and 48 h with the poly(catechol) and poly(*p*-phenylenediamine) that diffused from the fabrics to the culture media are depicted in Fig. 6. The data showed some variations in cell viability with the type of fabric and polymer; however, none of the raw fabrics elicit significant cytotoxicity when compared with the life control. Moreover, as the values of cytotoxicity obtained for the three types of fabrics were very similar among them, only one control of the raw fabrics was included in Fig. 6.

No cytotoxicity was observed for PET-coated samples for any of the tested conditions, while for the wool-coated fabrics, a significant decrease in cell viability was observed after 24 and 48 h of incubation. For these samples, only the poly(catechol) and poly(*p*-phenylenediamine) 1:10 dilutions did not affect the viability of fibroblasts. The high levels of coating obtained for wool and the lower washing fastness might help to explain these results. Despite the coating yield observed for this fabric being higher because of its porous fabric structure and inherent scale-shape, the fastness to washing was lower than that observed for the other two fabrics, as can be seen in Table S1. Thus, when in contact with the culture medium, the polymers tend to diffuse intensively to the medium, thus saturating it and leading to cytotoxicity.

With regard to the cotton fabric, only the poly(*p*-phenylenediamine) sample affected negatively the cell viability after 48 h of incubation. Yet, as for the wool fabrics, this effect was dependent on the polymer concentration present on the culture medium (no significant effect was found for the 1:2 dilution when compared with the life control).

4. Conclusions

PET, cotton, and wool fabrics were efficiently coated with poly (catechol) and poly(*p*-phenylenediamine). The coating was achieved by the laccase *in situ* polymerization of both catechol and *p*-phenylenediamine monomers assisted by HPH.

All fabrics coated with both polymers demonstrated antioxidant activity. Poly(catechol) revealed antioxidant activity up to 600 μg/mL of polymer, whereas poly(*p*-phenylenediamine) reached the saturation at 400 μg/mL of polymer used. Both polymers were able to confer antimicrobial activity to all the coated fabrics against gram-positive *S. aureus* and gram-negative *E. coli*.

The coating of PET and cotton fabrics with both polymers did not affect the viability of foreskin fibroblasts. The cells viability was, however, compromised by wool-coated fabrics because of the higher polymer diffusion from these textile substrates.

Our data allowed us to conclude that the methodology applied for fabric coating is a promising approach to obtain colored fabrics with antioxidant and antimicrobial activities, especially if PET and cotton are used as enzyme containers.

Funding

This study was supported by the Chinese Government Scholarship under China Scholarship Council [grant no. 201606790036], the Chinese Foundation Key Projects of Governmental Cooperation in International Scientific and Technological Innovation [grant no. 2016 YFE0115700], and the Portuguese Foundation for Science and Technology (FCT) under the scope of the strategic funding of UID/BIO/04469/2013 unit and COMPETE 2020 (POCI-01-0145-FEDER-006684), and BioTecNorte operation (NORTE-01-0145-FEDER-000004) funded by European Regional Development Fund under the scope of Norte2020 – Programa Operacional Regional do Norte. The work was also supported by the FCT – Fundação para a Ciência e a Tecnologia [grant nº SFRH/BD/121673/2016, SFRH/BPD/98388/2013, and IF/00186/2015].

Declaration of interest statement

The authors declare no competing financial and nonfinancial interests.

Appendix A. Supplementary data

Supplementary data to this article can be found online at https://doi.org/10.1016/j.reactfunctpolym.2018.11.015.

References

[1] D.S. Morais, R.M. Guedes, M.A. Lopes, Materials 9 (6) (2016) 498.
[2] R. Dastjerdi, M. Montazer, Colloids Surf. B: Biointerfaces 79 (1) (2010) 5–18.
[3] S. Shahidi, J. Wiener, Antimicrobial Agents, InTech, 2012.
[4] M. Majid, S. Samira, Photochem. Photobiol. 87 (4) (2011) 877–883.
[5] R. Purwar, M. Joshi, 2004.
[6] I. Cerkez, S.D. Worley, R.M. Broughton, T.S. Huang, React. Funct. Polym. 73 (11) (2013) 1412–1419.
[7] B. Izmaylov, D. Di Gioia, G. Markova, I. Aloisio, M. Colonna, V. Vasnev, React. Funct. Polym. 87 (2015) 22–28.
[8] O.Y. Jeong, J.C. Jin, S.S. Md, L.S. Yeong, I. Insik, P.S. Young, Surf. Interface Anal. 47 (2) (2015) 259–264.
[9] T.S. Sileika, H.D. Kim, P. Maniak, P.B. Messersmith, ACS Appl. Mater. Interfaces 3 (12) (2011) 4602–4610.
[10] B. Simoncic, B. Tomsic, Structures of novel antimicrobial agents for textiles - a review, Text. Res. J. 80 (16) (2010) 1721–1737.
[11] L.J. Bastarrachea, J.M. Goddard, Appl. Surf. Sci. 378 (2016) 479–488.

[12] J. Zhao, L. Ma, W. Millians, T. Wu, W. Ming, ACS Appl. Mater. Interfaces 8 (13) (2016) 8737–8742.
[13] F. Hui, C. Debiemme-Chouvy, Biomacromolecules 14 (3) (2013) 585–601.
[14] A. Chen, Starch 69 (2017) 1700046.
[15] M. Daglia, Curr. Opin. Biotechnol. 23 (2) (2012) 174–181.
[16] P. Camelia, N. Valentin, S. Georgeta, Compr. Rev. Food Sci. Food Saf. 16 (6) (2017) 1243–1268.
[17] D.-Y. Choi, Y.-J. Lee, J.T. Hong, H.-J. Lee, Brain Res. Bull. 87 (2) (2012) 144–153.
[18] K.B. Pandey, S.I. Rizvi, Oxidative Med. Cell. Longev. 2 (5) (2009) 270–278.
[19] A.M. Mileo, S. Miccadei, Oxidative Medicine and Cellular Longevity 2016, (2016).
[20] J.N. Jing Su, Fu Jiajia, Qiang Wang, Carla Silva, Artur Cavaco-Paulo Coloured and Low Conductive Fabrics by In Situ Laccase-Catalysed Polymerization Process Biochem, (2018).
[21] J. Su, J. Noro, A. Loureiro, M. Martins, N.G. Azoia, J. Fu, Q. Wang, C. Silva, A. Cavaco-Paulo, ChemCatChem 9 (20) (2017) 3888–3894.
[22] S.M. Daly, T.M. Przybycien, R.D. Tilton, Langmuir 21 (4) (2005) 1328–1337.
[23] R. Re, N. Pellegrini, A. Proteggente, A. Pannala, M. Yang, C. Rice-Evans, Free Radic. Biol. Med. 26 (9) (1999) 1231–1237.
[24] P.K. Jha, G.P. Halada, Chemi. Central J. 5 (1) (2011) 12.
[25] J. Su, T.G. Castro, J. Noro, J. Fu, Q. Wang, C. Silva, A. Cavaco-Paulo, Ultrason. Sonochem. 48 (2018) 275–280.
[26] T. Sulimenko, J. Stejskal, J. Prokeš, J. Colloid Interface Sci. 236 (2) (2001) 328–334.
[27] S. Dubey, D. Singh, R.A. Misra, Enzym. Microb. Technol. 23 (7–8) (1998) 432–437.
[28] M.R. Nabid, Z. Zamiraei, R. Sedghi, S. Nazari, Polym. Bull. 64 (9) (2010) 855–865.
[29] X.G. Li, M.R. Huang, R.F. Chen, Y. Jin, Y.L. Yang, J. Appl. Polym. Sci. 81 (13) (2001) 3107–3116.
[30] V. Shahedifar, A.M. Rezadoust, J. Reinf. Plast. Compos. 32 (10) (2013) 681–688.
[31] J. Anthoni, F. Lionneton, J.-M. Wieruszeski, J. Magdalou, J.-M. Engasser, L. Chebil, C. Humeau, M. Ghoul, Rasayan J Chem 1 (2008) 718–731.
[32] R.M. Desentis-Mendoza, H. Hernandez-Sanchez, A. Moreno, R.D.C. Emilio, L. Chel-Guerrero, J. Tamariz, M.E. Jaramillo-Flores, Biomacromolecules 7 (6) (2006) 1845–1854.
[33] M. Kurisawa, J.E. Chung, H. Uyama, S. Kobayashi, Biomacromolecules 4 (5) (2003) 1394–1399.
[34] L. Liu, J. Zhang, R.-C. Tang, React. Funct. Polym. 73 (11) (2013) 1559–1566.
[35] P.D. Askew, Chim. Oggi 27 (1) (2009) 16–20.
[36] Y. Gao, R. Cranston, Text. Res. J. 78 (1) (2008) 60–72.
[37] B. Caven, B. Redl, T. Bechtold, Text. Res. J.
[38] N. Abdelwahab, E. Al-Ashkar, M.A. El-Ghaffar, Trans. Nonferrous Metals Soc. China 25 (11) (2015) 3808–3819.
[39] S.L. Fink, B.T. Cookson, Infect. Immun. 73 (4) (2005) 1907–1916.
[40] J. Hasan, R. Crawford, E. Ivanova, 2013.
[41] G. Rudramurthy, M. Swamy, U. Sinniah, A. Ghasemzadeh, Molecules 21 (7) (2016) 836.
[42] E. Pinho, L. Magalhães, M. Henriques, R. Oliveira, Ann. Microbiol. 61 (3) (2011) 493–498.
[43] F.A.P. Scacchetti, E. Pinto, G.M.B. Soares, Proc Eng 200 (2017) 276–282.
[44] U.-C. Hipler, P. Elsner, Karger Medical and Scientific Publishers, (2006).